Electric Power Systems Research 196 (2021) 107283

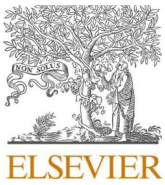

Contents lists available at ScienceDirect

Electric Power Systems Research

journal homepage: www.elsevier.com/locate/epsr

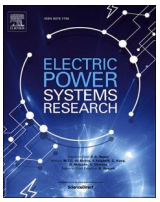

An upward negative lightning flash triggered by a distant +CG from a tall tower in Florida: Observations and modeling

V.A. Rakov [a], Y. Zhu [a,b,*], Z. Ding [a], M.D. Tran [a,c]

[a] Department of Electrical and Computer Engineering, University of Florida, Gainesville, FL 32611, United States
[b] Earth System Science Center, University of Alabama in Huntsville, Huntsville, AL, 35805, United States
[c] Rhombus Power Inc, Moffett Field, CA, 94035, United States

ARTICLE INFO

Keywords:
Upward negative lightning
Lightning-tall-object interaction
Induced effect of remote +CG
Upward positive leader
Subsequent stroke initiation
Electric field waveforms
Return-stroke models

ABSTRACT

We examined in detail the morphology and evolution of an upward negative flash initiated from a 257-m tower in Florida. High-speed video camera images and wideband electric field records, as well as ENTLN data, were used. The upward negative flash was induced (triggered) by a single-stroke 50-kA +CG that occurred about 45 km from the tower. The 257-m tower flash contained 6 leader/return stroke sequences and 1 attempted leader that almost terminated on the tower. All the leaders exhibited bidirectional extension. Electric field waveforms produced by the return strokes (measured at a distance of 8.8 km) were bipolar and abnormally narrow (exhibited earlier zero crossings). In order to examine the origin of the observed earlier zero crossings, we used two return-stroke models of transmission line type (MTLL and MTLE) to see what model input parameters are responsible for this feature. Within the limits of those models, the observed earlier zero crossings could be explained only by a narrow input current waveform or/and its fast amplitude decay with height.

1. Introduction

Tall objects are preferred targets for lightning strikes. Understanding of how lightning interacts with tall objects is important for characterizing the various lightning processes and improving lightning protection schemes. In contrast to short objects that experience only normal downward cloud-to-ground lightning, a tall object can initiate upward lightning whose initial leader develops from the object tip toward the overhead thundercloud. Berger and Vogelsanger [1] were apparently the first to suggest that the high electric field needed for the initiation of upward lightning is rapidly created by an in-cloud discharge, rather than being produced by the slower charge buildup in the cloud associated with the cloud electrification processes. Wang et al. [2] classified upward lightning into self-initiated flashes and other-triggered flashes (induced or triggered by another CG or IC flash), depending on whether or not there was nearby lightning activity immediately preceding the initiation of an upward leader from the object. The proportion of self--initiated and other-triggered (induced) lightning flashes apparently depends on storm type, its stage of development, and other factors and varies significantly in different studies [3–10]. Saba et al. [9] found that 100% of the 100 upward flashes they studied in Brazil and in the United States were triggered by other discharges. This is in contrast to the observation in Austria (Diendorfer et al. [10]) that 80% of the 307 upward flashes from the Gaisberg Tower were self-initiated. Results similar to those obtained for the Gaisberg tower were reported for the Peissenberg Tower in Germany and Santis Tower in Switzerland [6,8]. Schumann et al. [11,12] and Warner et al. [13] identified the following 3 processes that can trigger upward negative lightning flashes (defined as those transporting negative charge to ground): 1) positive return strokes (often referred to as +CGs), 2) negative parts of bidirectional leaders in IC or CG flashes, and 3) negative leaders associated with continuing current (CC) of +CG, serving to transport positive charge to ground.

This paper is based on (is an extended version of) the invited lecture given at SIPDA 2019 in Sao Paulo, Brazil. It integrates and expands three separate studies published in different journals by Zhu et al. [14–16]. We examined in detail the morphology and evolution of an upward negative flash terminated on a 257-m tower in Florida. High-speed video camera images and wideband electric field records, as well as ENTLN data, were used. The upward negative flash was induced (triggered) by a single-stroke 50-kA +CG that occurred about 45 km from the tower. The 257-m tower flash contained 6 leader/return stroke sequences and 1 attempted leader that almost terminated on the tower. The electromagnetic signatures of all six return strokes were abnormally narrow,

* Corresponding author.
E-mail address: yananzhu@ufl.edu (Y. Zhu).

https://doi.org/10.1016/j.epsr.2021.107283
Received 16 September 2020; Received in revised form 5 April 2021; Accepted 12 April 2021
0378-7796/© 2021 Elsevier B.V. All rights reserved.

compared to their counterparts for lightning strikes to ground or short grounded objects. Two approaches to return-stroke modeling aimed at reproduction of those signatures will be discussed.

2. Instrumentation

The LOG has been established in 2004 and is currently located on the roof of the five-story New Engineering Building on the campus of the University of Florida. The LOG includes a glass cupola providing over a 180° unobstructed view of the horizon. The cupola houses optical instrumentation, computers, and digitizing oscilloscopes, while the sensors are located on the roof, outside the cupola. Sensors currently used at LOG include electric field (E) antennas, electric field derivative (dE/dt) antennas, magnetic field derivative (dB/dt) antennas, and an x-ray detector. A total of four high-speed video cameras are presently installed at LOG. Two electric field measuring systems and one high-speed video camera that were used in the present study are described below. Further information on LOG can be found in the review paper by Rakov et al. [17]..

The electric field measuring systems include the low-gain electric field measuring system with RC decay time constant of $\tau = 10$ ms and the high-gain electric field measuring system with RC decay time constant of $\tau = 440$ μs. The bandwidths are 16 Hz to 10 MHz and 360 Hz to 10 MHz for the low-gain and high-gain systems, respectively. The record length for the field measuring systems was 1 s with 200 ms pretrigger. The electric field waveforms shown in this paper are not compensated for instrumental decay.

The Megaspeed HHC-X2 camera, equipped with a fish-eye (F-theta) lens to provide a wider field of view (about 185°), was operated at 1000 frames per second (fps) with 1 ms exposure time (no deadtime) and resolution of 832 × 600 pixels. The effect of fish-eye lens distortion was eliminated (compensated for) in calculating lightning channel lengths and extension speeds. The record length of the camera was 1.2 s with 200 ms pretrigger. All the lengths and speeds estimated from the optical records and presented in this paper are 2D.

Both the U.S. National Lightning Detection Network (NLDN) and Earth Networks Total Lightning Detection Network (ENLTN) recorded the 257-m tower flash. NLDN data were used to characterize the return strokes, while the ENTLN data were used to identify and characterize lightning activity (including that inside the cloud) preceding and leading to initiation of the upward negative flash. Radar reflectivity maps from the WSR-88D weather radar located in Jacksonville, Florida, 110 km northeast of the 257-m tower were used to show the meteorological (thunderstorm structure) context of the tower flash.

3. Observations

3.1. General description

The tower from which the upward negative lightning was initiated is a 257-m tall radio antenna tower (see Fig. 1) located in northwest Gainesville, Florida. On July 16, 2014, during the dissipating stage of a thunderstorm, this tower received 2 lightning strikes (labeled 1593 and 1594). Event 1593 was the upward negative flash triggered by a +CG at a distance of 45 km from the tower. It contained 6 leader/return stroke sequences terminated on the tower. Event 1594 occurred 8 min after event 1593 and was a downward, double-termination bipolar flash. Its first stroke was positive and terminated on a 60-m tower at a distance of 3.6 km from the 257-m tower and the following two leader/return stroke sequences all terminated on the 257-m tower. Both events (flashes) will be described in this section, but the rest of the paper is devoted entirely to event 1593. Data for event 1593 are much more informative, primarily because the upper part of the channel for all 6 strokes was optically imaged up to a height of about 10 km above the tower top, while for event 1594 the upper part of the channel was hidden inside the cloud.

Fig. 1. The 257-m tower (University Of Florida DBA = WUFT-TV/FM Cell Site) in Gainesville, Florida, located 8.8 km from the LOG. The geographical coordinates of the tower are found at http://www.cellreception.com/towers/details.php?id=1029807.

The NLDN-reported locations for the 8 negative strokes (6 in event 1593 and 2 in event 1594) and the 257-m tower location are shown in Fig. 2. The distances between NLDN-reported locations and the tower location ranged from 40 to 140 m, all being less than 200 m, the median error (assumed to be equal to the semi-major axis length of the location error ellipse) reported by the NLDN for each located event. The peak currents for the 8 negative return strokes are also listed in Fig. 2. They range from 5.7 to 20.7 kA with an arithmetic mean of 8.8 kA. Out of 8 negative strokes, 6 were misclassified by the NLDN as cloud discharges. The 2 correctly classified strokes were 1593–3 and 1593–4.

3.2. Sequence of events leading to the initiation of upward negative flash

Using high-speed optical images and electric field records obtained at the Lightning Observatory in Gainesville (LOG), Florida, we examined in detail the morphology and evolution of the upward negative flash (event 1593) containing 6 downward leader/upward return stroke sequences terminated on the 257-m tall tower (see Fig. 1) in Florida. This flash was unusual in that the upper part of its channel, normally hidden inside the cloud, was visible for each of its 6 strokes up to a height of about 10 km above the tower top. It was induced (triggered) by a single-stroke 50-kA +CG (positive cloud-to-ground flash) that occurred about 45 km from the tower and whose in-cloud part was optically detected to extend (primarily horizontally with a descending trend) toward the tower and appeared to stop at a height of about 3 km above the tower top, as seen in Fig. 3. The ENTLN and radar data (see Fig. 4) indicate that the +CG apparently originated from a relatively distant thunderstorm cell separated by a lower-reflectivity gap of about 15 km from the cell located above the tower. The distance from the tower to the LOG is 8.8

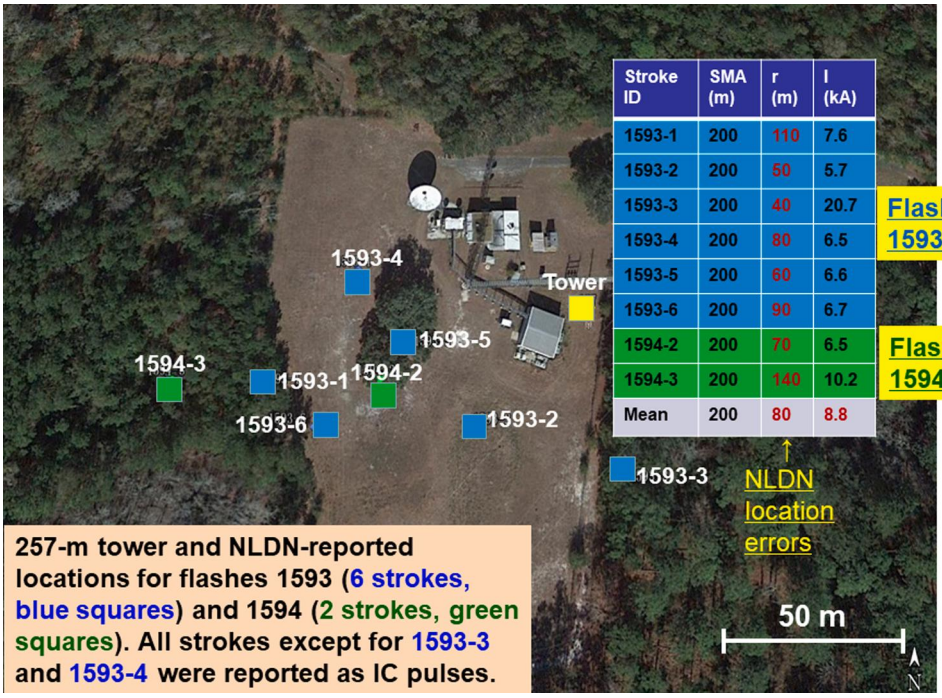

Fig. 2. Locations of strike points reported by the NLDN for 8 negative strokes (strokes 1 to 6 in flash 1593 and strokes 2 and 3 in flash 1594) terminated on the 257-m tower. Blue squares are the reported strike points for 6 strokes of flash 1593 and green squares are the reported strike points for 2 strokes of flash 1594. The yellow square is the location of the tower and the ground-truth location of the 8 strokes. SMA stands for the semi-major axis length of the NLDN-reported location error ellipse and r is the NLDN location error defined as the distance from the NLDN-reported location to the ground-truth location (yellow square). I is the NLDN-reported peak current.

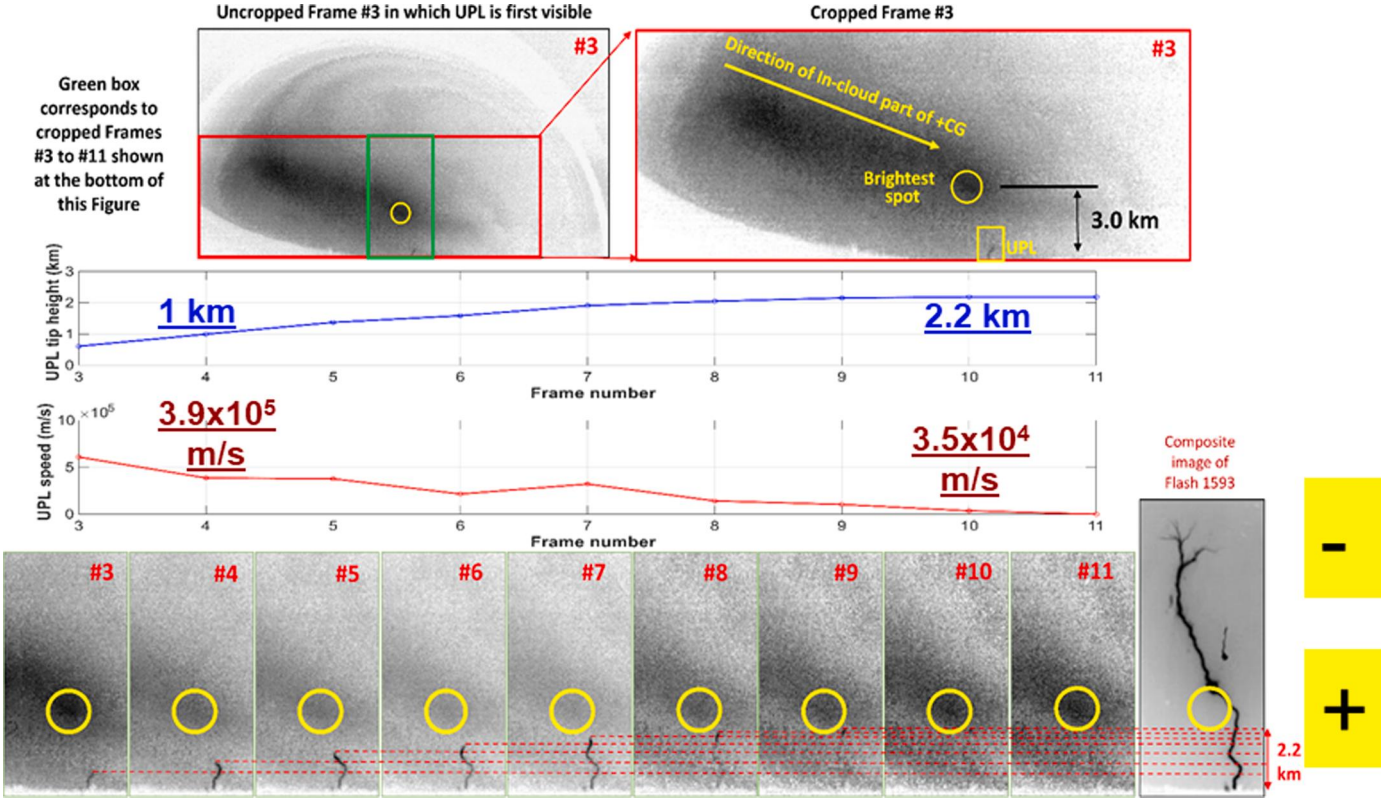

Fig. 3. Development of UPL initiated from the tower in response to the approaching in-cloud part of +CG (negative leader associated with +CG continuing current). Individual frames are numbered in the upper right corner. After frame #11, UPL became undetectable. The yellow circle represents the spot where the in-cloud negative leader associated with +CG continuing current ended. This spot was the brightest part of the in-cloud leader seen in frame #3.

km.

The in-cloud part of the +CG in effect transported negative charge to the cloud region above the tower and caused the initiation of an upward positive leader (UPL) from the tower. The UPL extended during about 8 ms to a height of about 2.2 km above the tower top, as the in-cloud part of the +CG (including its continuing current) faded away, and was followed by an initial continuous current (ICC). The UPL speed decreased from 3.9×10^5 m/s to 3.5×10^4 m/s. The ICC was associated with heavy

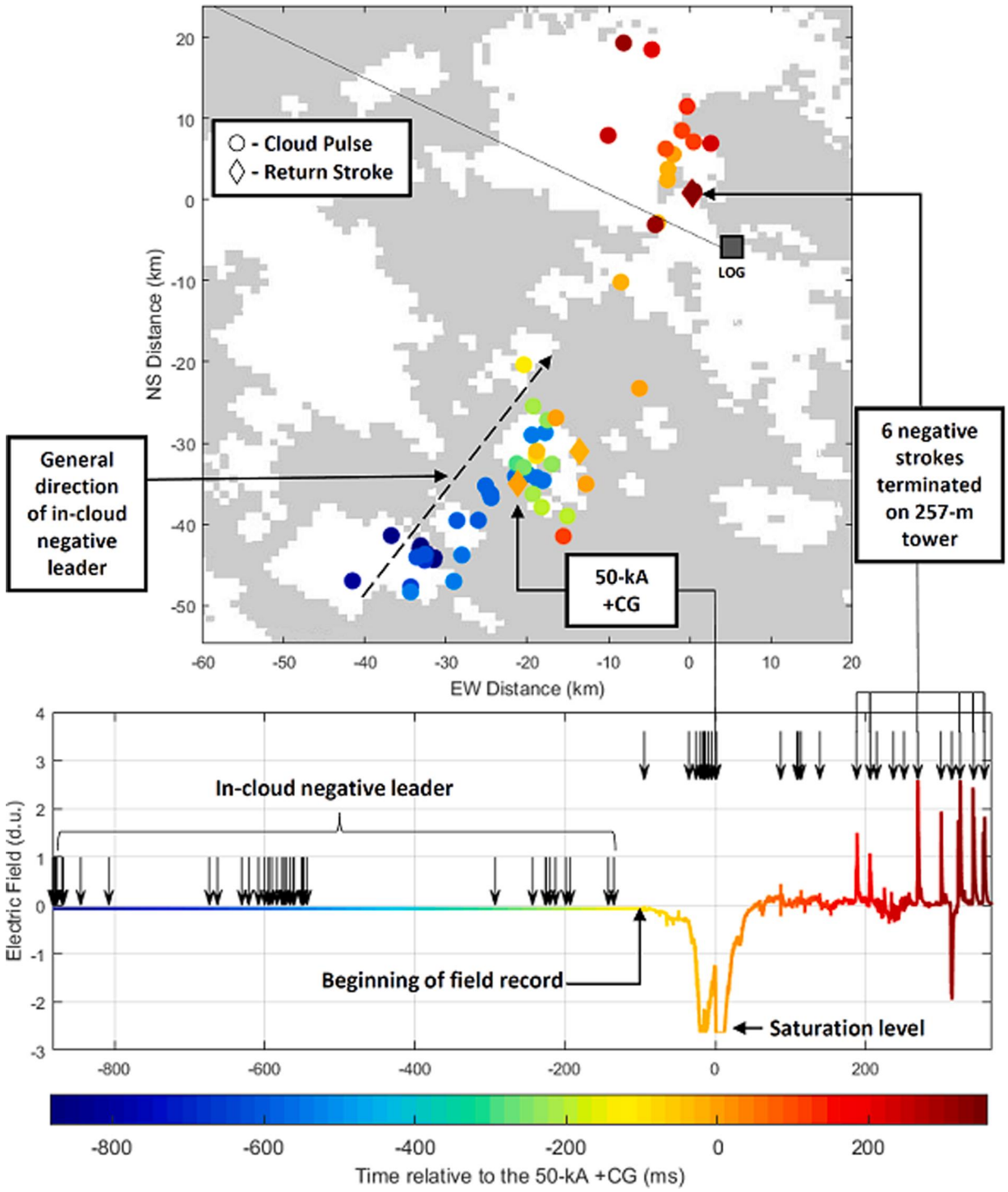

Fig. 4. (Top panel) ENTLN data (circles representing cloud pulses and diamonds representing return strokes) superimposed on a radar map showing only 2 levels of reflectivity, ≥35 dBZ (white areas) and <35 dBZ (gray areas). (Bottom panel) High-gain ($\tau = 440$ μs) electric field waveform measured at LOG. The time sequence of cloud pulses and return strokes (a total of 66) shown in the top panel is color-coded. Downward arrows in the bottom panel indicate the occurrence times of ENTLN-detected events.

branching in different directions. Most of the branches were faint and were revealed only via detection of moving bright leader tips and/or re-illumination of channels by transient recoil leaders. The branches extending predominantly upward were utilized by attempted downward leaders and leader/return-stroke sequences that occurred later in the flash. Schematic representation of the events inferred from Figs. 3 and 4 prior to the first leader/RS sequence is shown in Fig. 5.

Electric field records of the entire tower flash and its causative +CG, with all the significant events labeled, are shown in Fig. 6. Six negative downward-leader/upward-return-stroke sequences occurred 177 ms after UPL's becoming optically undetectable. We also examined one pronounced attempted leader (labeled AL in Fig. 6) that almost made contact with the tower.

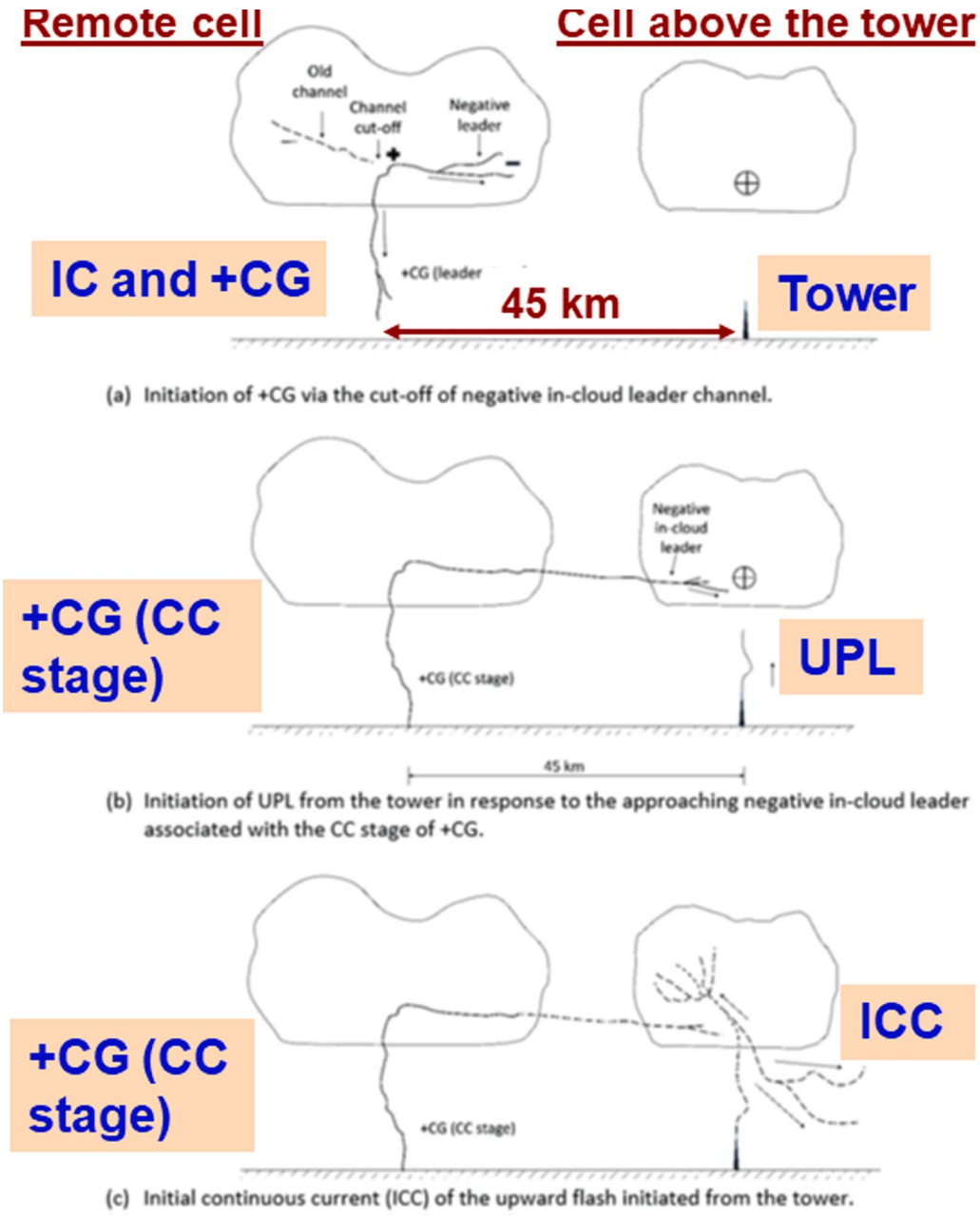

Fig. 5. Schematic representation of the events leading to the initiation of the upward positive leader (UPL) and initial continuous current (ICC), inferred from LOG and ENTLN records. The broken lines are used to show the parts of channels that were very faint and were revealed only via detection of moving leader tips and/or transients (recoil leaders) illuminating otherwise undetectable branches. There was evidence of persistent positive charge in the lower part of the thunderstorm cell located above the tower (deceleration and decay of UPL).

3.3. Initiation of subsequent strokes in the cloud (bidirectional leaders)

The initial frames showing the channels (including the upper parts normally hidden inside the cloud) of the six negative return strokes in flash 1593 are shown in Fig. 7. Each of them was initiated by what appeared to be a predominantly vertical bidirectional leader. Electric field signatures and corresponding video frames for strokes 1 and 4, as well as for the attempted leader labeled AL, are shown in Figs 8-10, respectively. Electric field signatures of bidirectional leaders were similar to those of K-changes. They appeared as ramps with durations of the order of 1 ms (from 1.3 to 3.0 ms with a mean of 1.7 ms, measured in high-gain electric field records that were compensated for instrumental decay), superimposed on which were often irregular microsecond-scale pulses and regular pulse bursts. In fact, the bidirectional leader is probably the process (or one of the processes) giving rise to K-changes in electric field records.

3.4. Unusual electric field signatures of return strokes

Electric field signatures of 6 return strokes in flash 1593 terminated on the tower were bipolar, which is not expected for strikes to ground at 8.8 km, and abnormally narrow: initial half-cycle durations ranged from 2.0 to 3.9 μs. These electric field signatures are shown in Fig. 11. The NLDN-reported peak currents were mostly relatively low, ranging from 5.7 to 20.7 kA with a mean of 9.0 kA. Without a tall strike object, typical return-stroke waveforms measured at a distance of 10 km or so are characterized by a sharp (essentially radiation) peak followed by an electrostatic ramp [18]. No zero-crossing in electric field waveform is expected for strikes to ground at 8.8 km. It is worth noting that lightning striking tall objects often produces electric field waveforms with first zero-crossing times ranging from 2 to 15 μs or so [14,19–22], which are significantly smaller than the typical values for strikes to ground ranging from 30 to 50 μs [23] [Ch.4].

As seen in Fig. 7, the upper end of the return-stroke channel of all 6 strokes in flash 1593 exhibited upward branching. The channel length

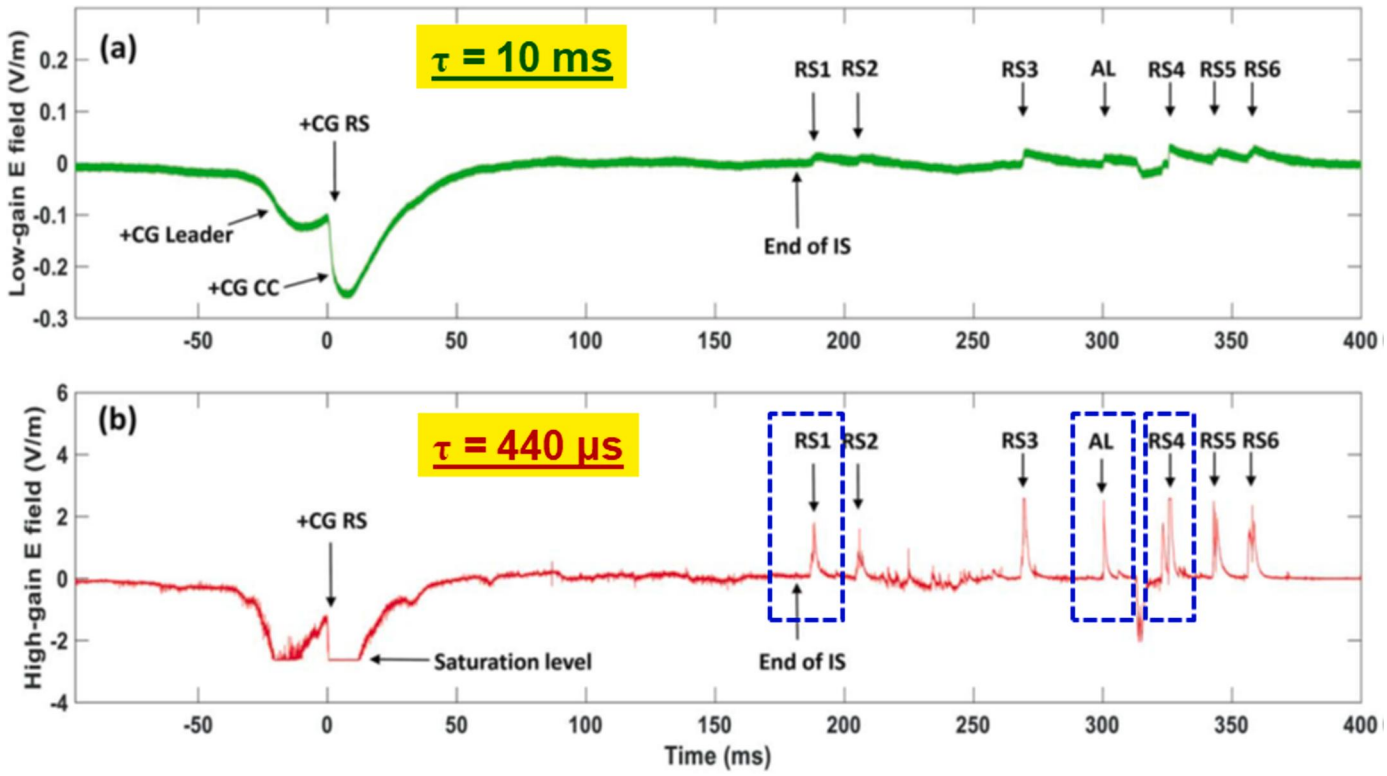

Fig. 6. (a) Low-gain (τ = 10 ms) and (b) high-gain (τ = 440 μs) records of the electric field produced by upward negative flash 1593, shown on a 500-ms time scale. IS, RS, and CC stand for the initial stage, return stroke, and continuing current, respectively. AL stands for the attempted leader. $t = 0$ corresponds to the onset of RS of +CG. UPL started 4 ms after the +CG RS onset. Electric field signatures of RS1, AL, and RS4 (boxed in (b)) and their corresponding high-speed video images are examined in Section 3.3.

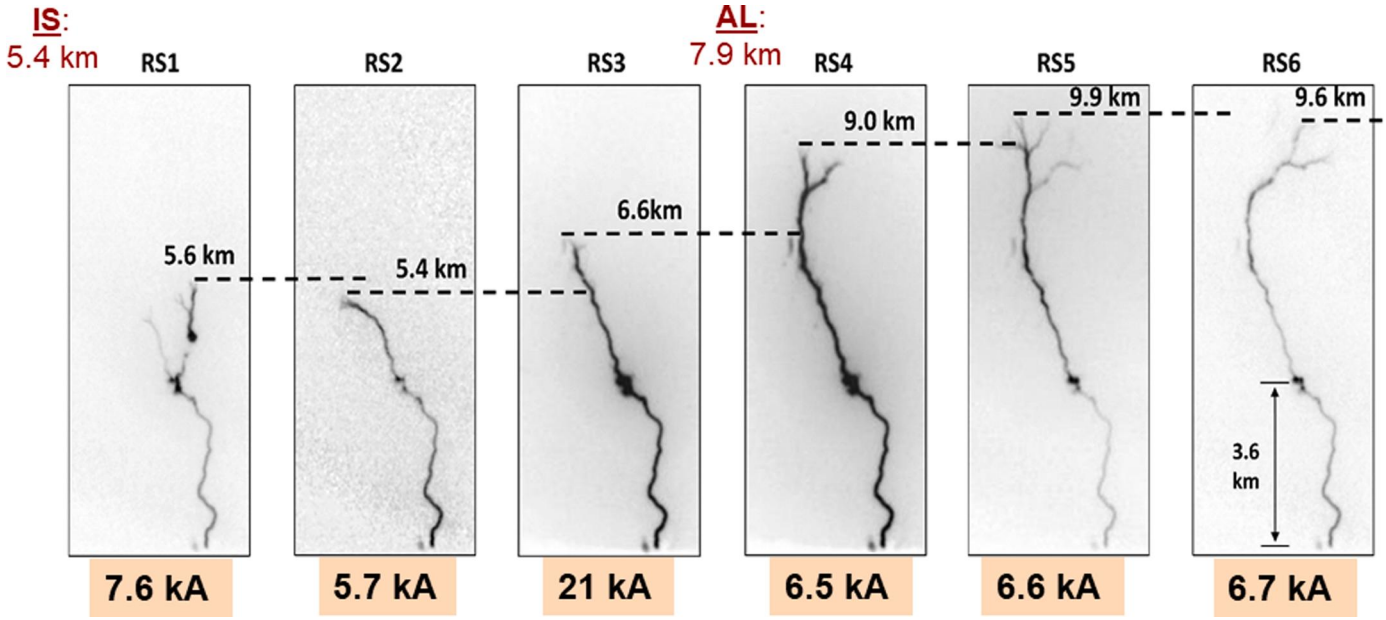

Fig. 7. Initial frames of each of the six return strokes (RS1 to RS6) of flash 1593. RS1 reached a height of 5.6 km versus 5.4 km, the maximum vertical extent of channels formed during the initial stage (IS). There was an attempted bidirectional leader (AL) between RS3 and RS4, whose upper end reached a height of 7.9 km. All the heights were estimated assuming that the channel was entirely in the plane that is perpendicular to the camera line of sight at $r = 8.8$ km from LOG. In reality, the upper part of the channel could be extending toward LOG. The upper cloud boundary height was 10 to 11 km.

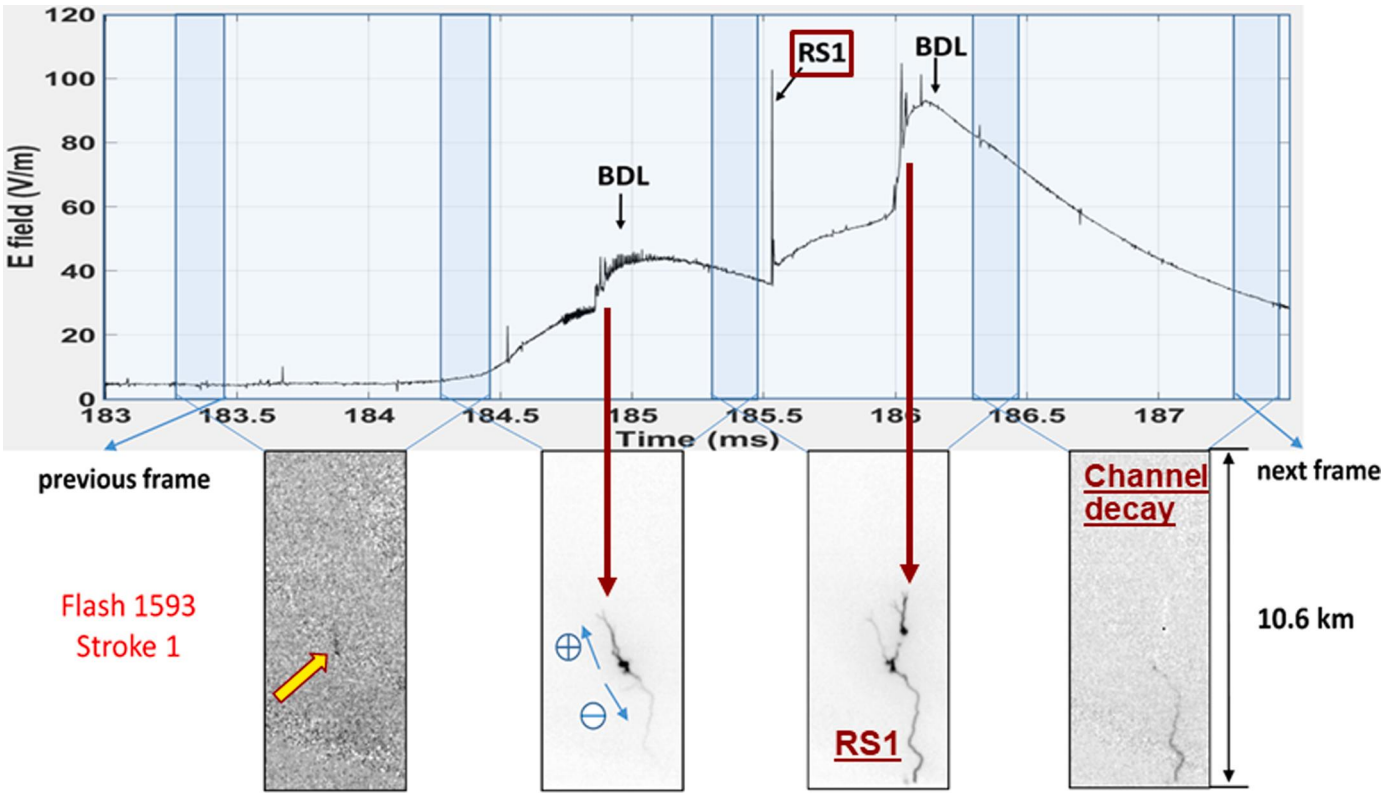

Fig. 8. High-gain (τ = 440 μs) electric field waveform of Stroke 1 aligned with its optical images (1 ms between frames). BDL stands for bidirectional leader. Alignment uncertainty is represented by darker areas in the electric field panel. The inferred bidirectional extension of leader is indicated by small arrows with the polarity of positive and negative ends being represented by encircled plus and minus signs.

tended to increase with increasing stroke order, up to a maximum height of about 10 km above the tower top. It is important to note, however, that the upper part of the channel could have extended toward LOG, in which case the maximum vertical extent would be smaller.

4. Modeling

4.1. Lightning/tower interaction model

In order to examine the origin of earlier zero-crossings (EZCs) observed in electric field signatures produced by lightning strikes to towers, we used the lumped voltage source excitation proposed by Baba and Rakov [24] and two return-stroke models of transmission line type (MTLL [25] and MTLE [26]), extended to include a tall strike object. The overall configuration includes two transmission lines, one representing the lightning channel and the other the strike object (tower), that are energized by a voltage source connected at the junction point between the two transmission lines (see Fig. 12). Current injected into both the channel and the tower is given by $I_{inj}=V_0/(Z_t+Z_{ch})$, where $V_0=Z_{ch}I_{sc}(h,t)$ is the voltage at the source terminals. Other symbols are explained below.

The distributions of current along the tower and along the lightning channel are given by Eqs. (1) and 2, respectively.

Along the tower ($0\le z'\le h$),

$$I(z',t)=\frac{1-\rho_t}{2}\sum_{n=0}^{\infty}\begin{bmatrix}\rho_g^n\rho_t^n I_{sc}\left(h,\ t-\dfrac{h-z'}{c}-\dfrac{2nh}{c}\right)\\ +\rho_g^{n+1}\rho_t^n I_{sc}\left(h,\ t-\dfrac{h+z'}{c}-\dfrac{2nh}{c}\right)\end{bmatrix}\quad 0\le z'\le h \tag{1}$$

Along the lightning channel ($z'\ge h$),

$$I(z',t)=\frac{1}{2}\begin{bmatrix}P(z'-h)\left(I_{sc}\left(h,\ t-\dfrac{z'-h}{v}\right)-\rho_t I_{sc}\left(h,\ t-\dfrac{z'-h}{v}\right)\right)\\ +(1-\rho_t)(1+\rho_t)\sum_{n=1}^{\infty}\rho_g^n\rho_t^{n-1}I_{sc}\left(h,\ t-\dfrac{z'-h}{v}-\dfrac{2nh}{c}\right)\end{bmatrix}\quad z'\ge h \tag{2}$$

where n is the number of reflections occurring between the top and bottom of the tower, h is the height of the tower, v is the speed of current wave traveling upward in the lightning channel, $P(z'-h)$ is the current attenuation function, and I_{sc} is the lightning short-circuit current, which is defined by Baba and Rakov [24] as the lightning current that would be measured at an ideally grounded object of negligible height. Note that in Eq. (2) above we fixed a misprint in Eq. (2) of Zhu et al. [15], where the attenuation function was applied only to the first term. For MTLE, $P(z'-h)=\exp(-(z'-h)/\lambda)$,where λ is the current decay height constant (or attenuation distance) and for MTLL, $P(z'-h)=1-(z'-h)/(H-h)$,where H is the lightning channel top height above ground. ρ_g and ρ_t are the current reflection coefficients at the tower bottom and tower top, respectively, which can be expressed as

$$\rho_g=\frac{Z_t-Z_g}{Z_t+Z_g} \tag{3}$$

$$\rho_t=\frac{Z_t-Z_{ch}}{Z_t+Z_{ch}} \tag{4}$$

where Z_t, Z_g, and Z_{ch} are the characteristic impedance of the tower, grounding impedance, and equivalent impedance of the lightning channel, respectively. Note that $(1-\rho_t)/2=Z_{ch}/(Z_t+Z_{ch})$. In this study, the top of lightning channel was assumed to be 5 km above ground.

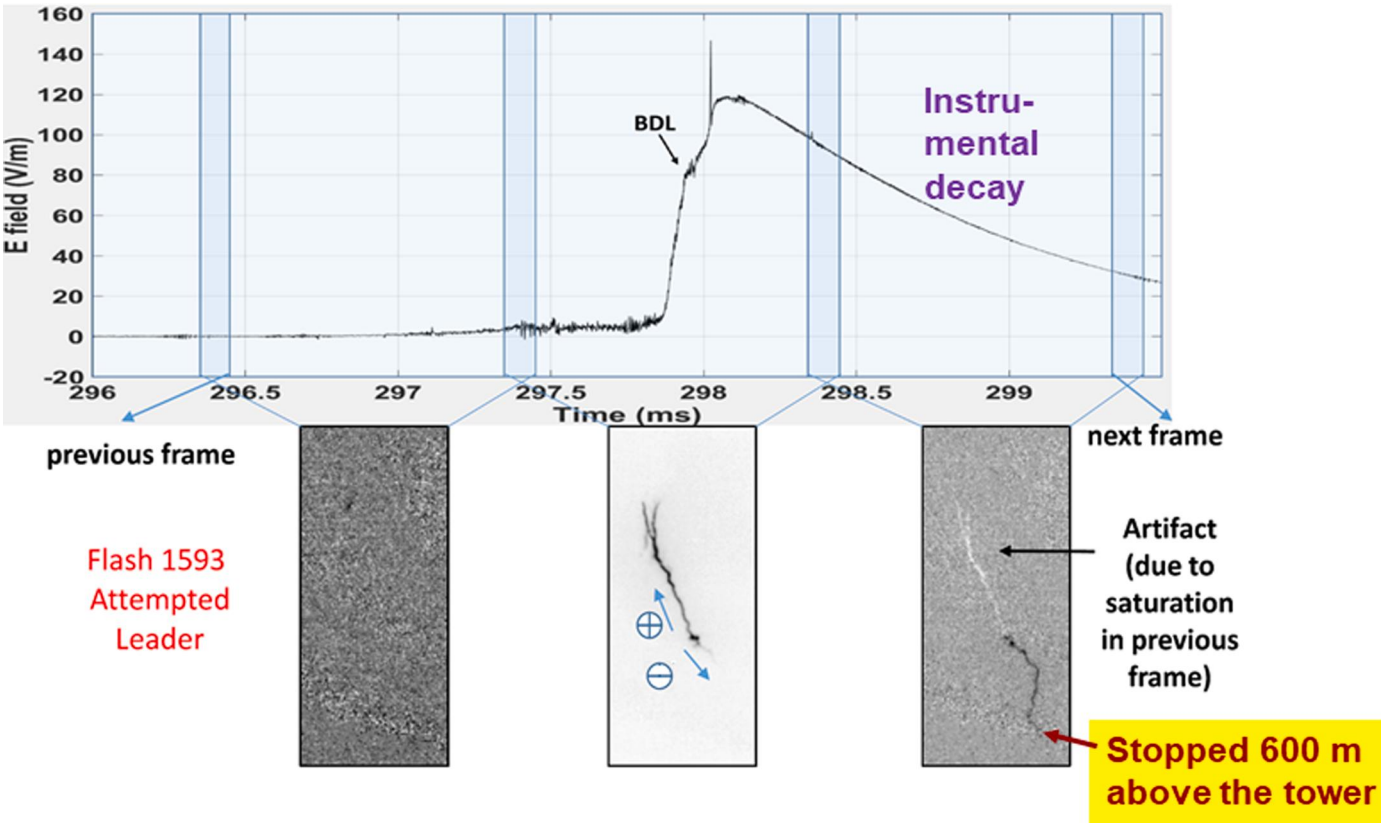

Fig. 9. High-gain (τ = 440 μs) electric field waveform of AL between Strokes 3 and 4 aligned with its optical images (1 ms between frames). BDL stands for bidirectional leader. Alignment uncertainty is represented by darker areas in the electric field panel. The inferred bidirectional extension of leader is indicated by small arrows with the polarity of positive and negative ends being represented by encircled plus and minus signs.

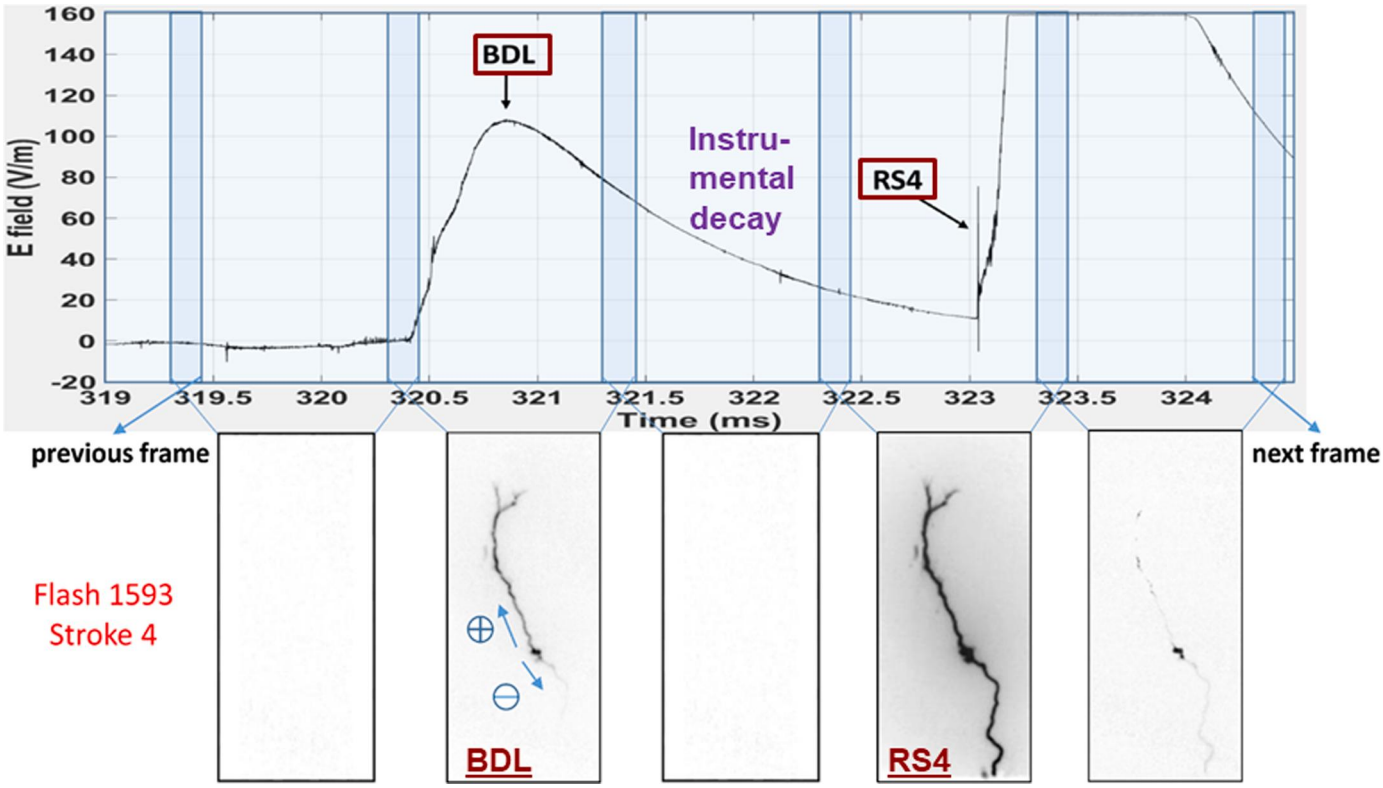

Fig. 10. High-gain (τ = 440 μs) electric field waveform of Stroke 4 aligned with its optical images (1 ms between frames). BDL stands for bidirectional leader. Alignment uncertainty is represented by darker areas in the electric field panel.

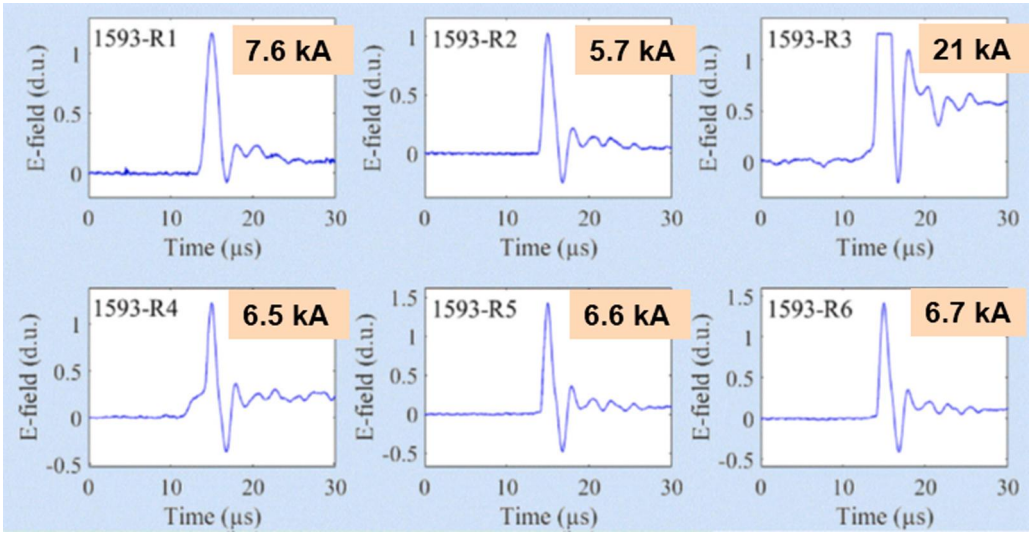

Fig. 11. Electric field signatures of 6 negative return strokes in flash 1593 terminated on the tower. The peak of the 1593-R3 waveform is clipped due to saturation.

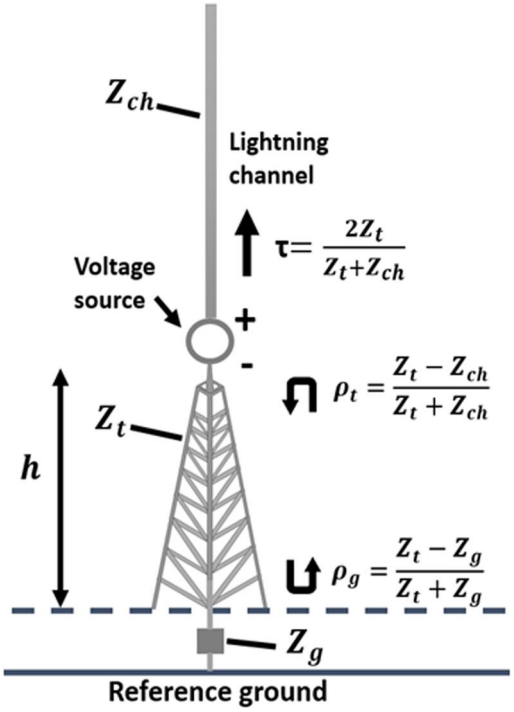

Fig. 12. Transmission line representation of lightning strike to a tall object.

The expression for electric field produced by an infinitesimal vertical dipole given by Uman et al. [27] and integration over the lightning channel and over the tower were used to compute the vertical electric fields presented below.

4.2. Conditions that can produce early zero-crossing in field waveforms

In this section, we examine via modeling the conditions that can cause the EZC in electric field waveforms. One question to answer is whether the traditional return-stroke models extended to include a tall strike object can explain the observed EZC field waveforms. We used two return-stroke models (MTLE and MTLL) and different channel base (input) current waveforms to answer this question. In Fig. 13, we demonstrate that the traditional MTLE model with $\lambda = 2$ km does not reproduce the EZC, but it does if λ is reduced to 100 m. Similarly, the traditional MTLL model does not work with "normal" channel-base current waveform, but does predict EZC when a narrower current waveform is used. Fig. 13a shows the typical channel-base current waveform (not influenced by reflections) of a subsequent stroke, which is expressed by the Heidler function [Heidler, 1985]. Parameters for the Heidler function used here were the same as those specified in IEC 62305–1, except for the current peak, which was reduced here to 10 kA from the 50 kA in IEC 62305–1. In this study, the value of n was set to 10 and η to 0.993, with T and τ being 0.454 μs and 143 μs, respectively, as per IEC 62305–1. Reflection coefficients at the tower top and bottom were set to −0.5 and 1, respectively, and return-stroke speed was set to one-half of the speed of light. These (or similar) values are widely used in studies of lightning interaction with tall objects (e.g. [30–32],). Influence of the variation of reflection coefficients and return-stroke speed on electric field waveforms is shown, for example, in Section 4 of [15].

It is clear from Fig. 13 that the early zero crossing occurs in (c) and (f), but not in (b) and (d). Thus, the observed narrow field signatures cannot be reproduced by traditional return-stroke models [23, Ch. 12] and require a narrower input current waveform or/and its faster decay with height. This conclusion is limited by the model we employed for computing electric fields (see Fig. 12). Beyond the limits of our model, other explanations of EZC are possible (e.g., lightning channel turning horizontal at higher altitudes, the geometry considered by Saito et al. [28] and Araki et al. [29]). Clearly, further research is needed.

4.3. Modeling of lightning events terminated on the 257-m tower

The narrow (initial half-cycle width ranging from 2.0 to 3.9 μs) bipolar electric field waveforms produced by lightning striking the 257-m tower in Florida were reproduced using two approaches. In the first one, we employed a typical channel-base (input) current waveform (HPW ranging from 36 to 106 μs) and the MTLE (exponential current decay with height) model with a very small value of λ (tens to hundreds of meters) . The input current pulses and computed electric field waveforms for the first approach are shown in Fig. 14. In the second approach, we used a narrow impulsive current component (HPW ranging from 1.0 to 2.3 μs) followed by a steady-level tail as the channel-base (input) current waveform and the MTLL (linear current decay with height) model. The input current pulses and computed electric field waveforms for the second approach are shown in Fig. 15. In both approaches, the computed electric field waveforms matched well the corresponding measured waveforms for the initial half-cycle and opposite-polarity overshoot, while the oscillatory tail in the measured field waveforms was not well reproduced.

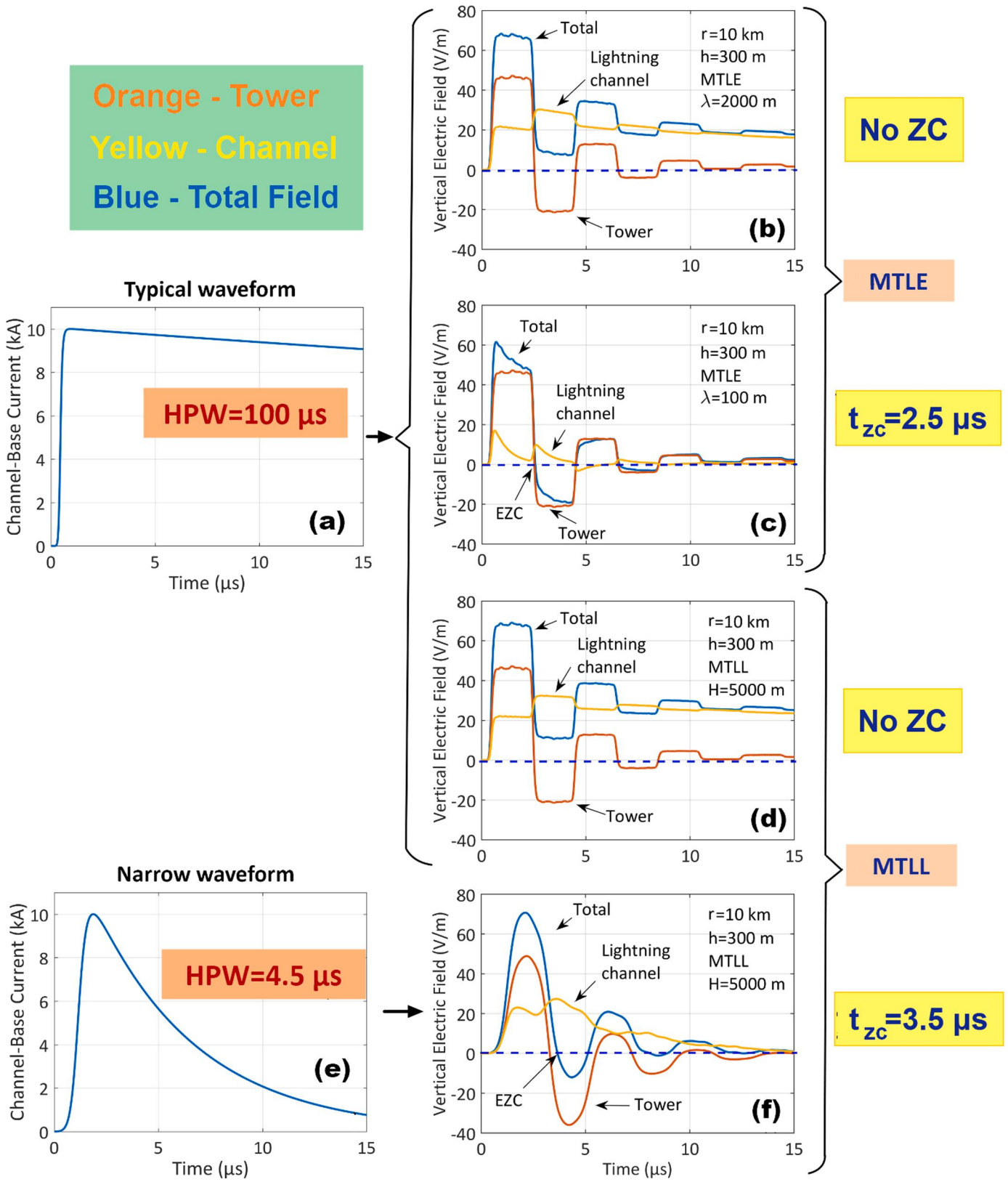

Fig. 13. Dependence of the vertical electric field at $r = 10$ km on the waveshape of channel-base current and return-stroke model for lightning strikes to a 300-m tower. **(a)** Current waveform recommended for subsequent strokes by IEC 62305–1, except for its magnitude, which was scaled down by a factor of 5. **(b)** and **(c)** Electric field waveforms computed using the channel-base current shown in (a) and the MTLE model with λ=2000 m and λ=100 m, respectively. **(d)** Electric field computed using the channel-base (input) current waveform shown in (a) and the MTLL model. **(e)** and **(f)** Channel-base (input) current waveform with considerably faster decay (half-peak width = 4.5 μs vs. 100 μs in (a)) and its corresponding electric field waveform computed using the MTLL model. Besides the total electric field, contributions from the tower (bipolar) and from the lightning channel (unipolar) are shown in (b), (c), (d), and (f).

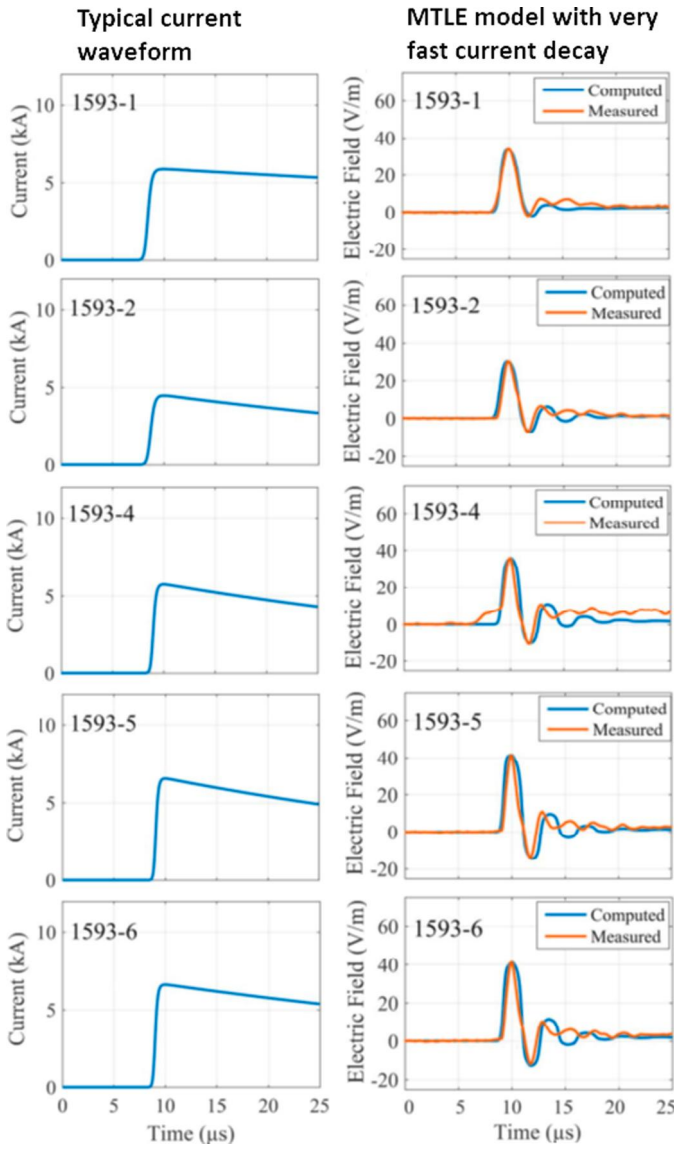

Fig. 14. (Left column) Channel-base (input) current waveforms, represented by Heidler functions, that were used for computing (based on the MTLE model) the electric field waveforms in the right column. (Right column) Measured and computed electric field waveforms at 8.8 km. In each case, the current waveforms and value of λ were adjusted to achieve the best match between the computed and measured electric field waveforms. A complete list of adjustable parameters is found in Table 3 of [15].

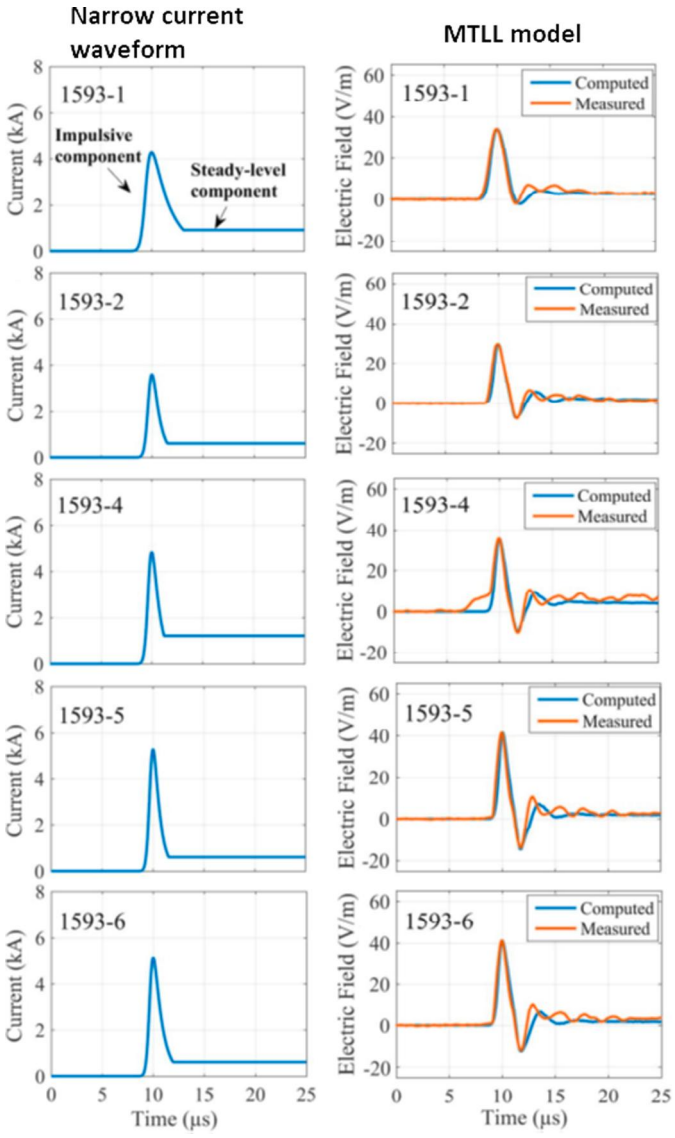

Fig. 15. (Left column) Channel-base current (input) waveforms that were used for computing (based on the MTLL model) the electric field waveforms shown in the right column. Steady-level components with magnitudes ranging from 200 to 1200 A were attached to the tail of the impulsive current components. (Right column) Measured and computed electric field waveforms at 8.8 km. The current waveforms were adjusted to achieve the best match between the computed and measured electric field waveforms. A complete list of adjustable parameters is found in Table 4 of [15].

Clearly, the narrow current pulses in the left column of Fig. 15 are not representative of lightning return strokes and indicative of a small charge involved in the leader/return stroke sequence. In fact, those events might not be regular strokes but a by-product of a relatively small, K-change type in-cloud discharge that is barely capable of touching the tower because of (1) the electric field enhancement by the tall tower, (2) the presence of remnants of the upward positive leader (labeled UPL in Fig. 3), and (3) the apparent presence of remnants of the in-cloud part of the initiating +CG (see yellow circle in Fig. 3 and the pesistent bright spot in Fig. 7) at relatively low altitudes of 2–4 km. All these conditions probably serve to reduce the minimum charge required to drive the leader all the way to the grounded object, which should lead to a narrower return-stroke current pulse.

In summary, the narrow bipolar signatures can be reproduced using the MTLE model with a typical channel-base current waveform and a very small attenuation distance λ (tens to hundresds of meters) or the MTLL model with a narrow current waveform (half-peak width ranging from 1.0 to 2.3 μs) followed by a steady-level tail.

5. Summary and concluding remarks

1 We examined in detail the morphology and evolution of an upward negative flash containing 6 downward leader/upward RS sequences terminated on a 257-m-tall tower in Florida. This flash was triggered by a single-stroke 50-kA +CG that occurred about 45 km from the tower.
2 Each of the six leader/RS sequences was initiated by a bidirectional leader utilizing the remnants of the branches created during the initial stage (UPL + ICC). Electric field signatures of bidirectional leaders that initiated RSs and the one failing to do so were similar to (or same as) K-changes.

3 The upper end of the RS channel in all six cases exhibited upward branching and tended to extend to higher altitudes or/and move closer to the camera with increasing stroke order.
4 For all the strokes that terminated on the 257-m tower (located 8.8 km from LOG), the return-stroke electric field signatures were very narrow (zero-crossing times less than 4 μs) bipolar pulses with damped oscillatory tails, very different from the signatures of return strokes in lightning strikes to ground or shorter grounded objects.
5 The observed narrow electric field signatures can be reproduced using
   (a) the MTLE (exponential current decay with height) model with a typical channel-base current waveform and a very small attenuation distance λ (tens to hundreds of meters) and
   (b) the MTLL (linear current decay with height) model with a narrow current waveform (half-peak width ranging from 1.0 to 2.3 μs) followed by a steady-level tail.
6 The narrow input current pulse must be due to a small charge involved. The strokes presented here might each be just a byproduct of small, K-change type in-cloud discharge that was barely capable of touching the tower. They would probably not occur (remain in the cloud) if the tall tower were not present. Further research is needed to better understand this phenomenon.
7 The results of this study will be useful in improving our understanding of the interaction of lightning with tall man-made objects, including wind turbines. This, in turn, will help engineers in designing better lightning protection means, as well as those developing advanced approaches to the classification of lightning events terminating on tall objects and estimation of their peak currents for modern lightning locating systems.

Credit author statement

All authors contributed to discussion of the results and preparation of the manuscript

CRediT authorship contribution statement

V.A. Rakov: Conceptualization, Writing – original draft, Writing – review & editing, Supervision, Funding acquisition. **Y. Zhu:** Conceptualization , Writing – original draft, Writing – review & editing, Formal analysis, Methodology, Software. **Z. Ding:** Formal analysis, Visualization. **M.D. Tran:** Data curation.

Declaration of competing interest

The authors declare that they have no known competing financial interests or personal relationships that could have appeared to influence the work reported in this paper.

Acknowledgement

This research was supported in part by NSF grant AGS-1701484. The authors would like to thank Michael Stock for providing ENTLN data and Amitabh Nag for providing the NLDN data used in this paper. We also thank Bruno Medina for his help with the interpretation of radar data.

References

[1] K. Berger, E. Vogelsanger, New results of lightning observations, in: Planet. Electrodyn., 1969: pp. 489–510.
[2] D. Wang, N. Takagi, T. Watanabe, H. Sakurano, M. Hashimoto, Observed characteristics of upward leaders that are initiated from a windmill and its lightning protection tower, Geophys. Res. Lett. 35 (2008) L02803, https://doi.org/10.1029/2007GL032136.
[3] N. Takagi, D. Wang, Characteristics of Winter Lightning that Occurred on a Windmill and its Lightning Protection Tower, IEEJ Trans. Power Energy. 131 (2011) 532–535, https://doi.org/10.1541/ieejpes.131.532.
[4] T.A. Warner, K.L. Cummins, R.E. Orville, Upward lightning observations from towers in Rapid City, South Dakota and comparison with National Lightning Detection Network data, 2004-2010, J. Geophys. Res. Atmos. 117 (2012), https://doi.org/10.1029/2012JD018346.
[5] H. Zhou, G. Diendorfer, R. Thottappillil, H. Pichler, M. Mair, Measured current and close electric field changes associated with the initiation of upward lightning from a tall tower, J. Geophys. Res. Atmos. 117 (2012) 1–9, https://doi.org/10.1029/2011JD017269.
[6] F. Heidler, M. Manhardt, K. Stimper, Self-initiated and other-triggered positive upward lightning measured at the Peissenberg Tower, Germany, 2014 Int. Conf. Light. Prot. ICLP 2014 (2014) 157–166, https://doi.org/10.1109/ICLP.2014.6973113.
[7] R. Jiang, X. Qie, Z. Wu, D. Wang, M. Liu, G. Lu, D. Liu, Characteristics of upward lightning from a 325-m-tall meteorology tower, Atmos. Res. 149 (2014) 111–119, https://doi.org/10.1016/j.atmosres.2014.06.007.
[8] A. Smorgonskiy, A. Tajalli, F. Rachidi, M. Rubinstein, G. Diendorfer, H. Pichler, An analysis of the initiation of upward flashes from tall towers with particular reference to Gaisberg and Säntis Towers, J. Atmos. Solar-Terrestrial Phys. 136 (2015) 46–51, https://doi.org/10.1016/j.jastp.2015.06.016.
[9] M.M.F. Saba, C. Schumann, T.A. Warner, M.A.S. Ferro, A.R. de Paiva, J. Helsdon, R.E. Orville, Upward lightning flashes characteristics from high-speed videos, J. Geophys. Res. Atmos. 121 (2016) 8493–8505, https://doi.org/10.1002/2016JD025137.
[10] G. Diendorfer, H. Pichler, D. Lackner, Self-initiated versus Nearby-lightning-triggered Upward Flashes at the Gaisberg Tower (2005 - 2015), in: 25th Int. Conf. Light. Detect., Fort Lauderdale, Florida, USA, 2018.
[11] C. Schumann, M.M.F. Saba, T.A. Warner, M.A.S. Ferro, J.H. Helsdon, R. Thomas, R. E. Orville, On the triggering mechanisms of upward lightning, Sci. Rep. 9 (2019) 1–9, https://doi.org/10.1038/s41598-019-46122-x.
[12] C. Schumann, M.M.F. Saba, T.A. Warner, Upward flashes triggering mechanisms, in: 2017 Int. Symp. Light. Prot. (XIV SIPDA), Natal, Brazil, 2017.
[13] T.A. Warner, A. Ballweber, R. Lueck, J.H. Helsdon, C. Schumann, M.M.F. Saba, J. Tilles, R.J. Thomas, R.E. Orville, Upward lightning triggering study (UPLIGHTS): project summary and initial findings, in: 25th Int. Conf. Light. Detect., Fort Lauderdale, Florida, USA, 2018.
[14] Y. Zhu, V.A. Rakov, M.D. Tran, Optical and electric field signatures of lightning interaction with a 257-m tall tower in Florida, Electr. Power Syst. Res. 153 (2017) 128–137, https://doi.org/10.1016/j.epsr.2016.08.036.
[15] Y. Zhu, V.A. Rakov, M.D. Tran, W. Lyu, D.D. Micu, A modeling study of narrow electric field signatures produced by lightning strikes to tall towers, J. Geophys. Res. Atmos. 123 (2018), https://doi.org/10.1029/2018JD028916, 10,260-10,277.
[16] Y. Zhu, Z. Ding, V.A. Rakov, M.D. Tran, Evolution of an upward negative lightning flash triggered by a distant +CG from a 257-m-tall tower, including initiation of subsequent strokes, Geophys. Res. Lett. 46 (2019) 7015–7023, https://doi.org/10.1029/2019GL083274.
[17] V.A. Rakov, E.A. Mareev, M.D. Tran, Y. Zhu, N.A. Bogatov, A.Y. Kostinskiy, V. S. Syssoev, W. Lyu, High-speed optical imaging of lightning and sparks: some recent results, IEEJ Trans. Power Energy. 138 (2018) 321–326, https://doi.org/10.1541/ieejpes.138.321.
[18] Y.T. Lin, M.A. Uman, J.A. Tiller, R.D. Brantley, W.H. Beasley, E.P. Krider, C. D. Weidman, Characterization of lightning return stroke electric and magnetic fields from simultaneous two-station measurements, J. Geophys. Res. 84 (1979) 6307, https://doi.org/10.1029/JC084iC10p06307.
[19] M. Ishii, M. Saito, Lightning electric field characteristics associated with transmission-line faults in winter, IEEE Trans. Electromagn. Compat. 51 (2009) 459–465, https://doi.org/10.1109/TEMC.2009.2025496.
[20] D. Pavanello, F. Rachidi, M. Rubinstein, J.L. Bermudez, W. Janischewskyj, V. Shostak, C.A. Nucci, A.M. Hussein, J.S. Chang, On return stroke currents and remote electromagnetic fields associated with lightning strikes to tall structures: 1. Computational models, J. Geophys. Res. Atmos. 112 (2007), https://doi.org/10.1029/2006JD007958.
[21] H. Pichler, G. Diendorfer, M. Mair, Some parameters of correlated current and radiated field pulses from lightning to the Gaisberg tower, IEEJ Trans. Electr. Electron. Eng. 5 (2010) 8–13, https://doi.org/10.1002/tee.20486.
[22] T. Wu, S. Yoshida, T. Ushio, Z. Kawasaki, Y. Takayanagi, D. Wang, Large bipolar lightning discharge events in winter thunderstorms in Japan, J. Geophys. Res. Atmos. 119 (2014) 555–566, https://doi.org/10.1002/2013JD020369.
[23] V.A. Rakov, M.A. Uman, Lightning: Physics and Effects, Cambridge University Press, New York, 2003.
[24] Y. Baba, V.A. Rakov, On the use of lumped sources in lightning return stroke models, J. Geophys. Res. Atmos. 110 (2005) 1–10, https://doi.org/10.1029/2004JD005202.
[25] V.A. Rakov, A.A. Dulzon, Calculated electromagnetic fields of lightning return stroke, Tekh. Elektrodinam. 1 (1987) 87–89.
[26] C.A. Nucci, C. Mazzetti, F. Rachidi, M. Ianoz, On lightning return stroke models for LEMP calculations, in: 19th Int. Conf. Light. Prot., Graz, Austria, 1988.
[27] M.A. Uman, D.K. McLain, E.P. Krider, The electromagnetic radiation from a finite antenna, Am. J. Phys. 43 (1975) 33, https://doi.org/10.1119/1.10027.

[28] M. Saito, T. Miki, T. Shindo, H. Motoyama, M. Ishii, T. Sonehara, H. Taguchi, A. Tajima, A. Fujisawa, Reproduction of electromagnetic field waveforms of subsequent return strokes hitting Tokyo Skytree over lossy ground, IEEJ Trans. Power Energy. 135 (2015) 472–478, https://doi.org/10.1541/ieejpes.135.472.
[29] S. Araki, Y. Nasu, Y. Baba, V.A. Rakov, M. Saito, T. Miki, 3-D finite difference time domain simulation of lightning strikes to the 634-m Tokyo Skytree, Geophys. Res. Lett. 1–8 (2018), https://doi.org/10.1029/2018GL078214.
[30] V.A. Rakov, Transient response of a tall object to lightning, IEEE Trans. Electromagn. Compat. 43 (2001) 654–661, https://doi.org/10.1109/15.974646.
[31] Y. Baba, V.A. Rakov, Lightning electromagnetic environment in the presence of a tall grounded strike object, J. Geophys. Res. D Atmos. 110 (2005) 1–18, https://doi.org/10.1029/2004JD005505.
[32] D. Pavanello, F. Rachidi, V.A. Rakov, C.A. Nucci, J.L. Bermudez, Return stroke current profiles and electromagnetic fields associated with lightning strikes to tall towers: comparison of engineering models, J. Electrostat. 65 (2007) 316–321, https://doi.org/10.1016/j.elstat.2006.09.014.